


TRANSVERSELY ISOTROPIC ELASTOPLASTIC BEHAVIOUR IN A MECHANICALLY LOADED ROTATING DISK

TRANSVERZALNO IZOTROPNO ELASTOPLASTIČNO PONAŠANJE KOD MEHANIČKI OPTEREĆENOG ROTIRAJUĆEG DISKA


Originalni naučni rad / Original scientific paper
Rad primljen / Paper received: 7.06.2023

Adresa autora / Author's address:

¹⁾ Department of Mathematics, Career point University Hamirpur, Himachal Pradesh, India

²⁾ Department of Mathematics, Faculty of Science and Technology, ICFAI University, Himachal Pradesh, India  0000-0001-8119-2697, *email: pankaj_thakur15@yahoo.co.in

³⁾ Department of Mathematics, Govt. Degree College Nalagarh, Himachal Pradesh, India

⁴⁾ Department of Mathematics, ICFAI University, Himachal Pradesh, India  0009-0009-0266-2298

Keywords

- stresses
- disk
- beryl
- magnesium
- angular speed

Abstract

This article deals with the study of transversely isotropic elastoplastic behaviour in a mechanical loaded rotating disk by using transition theory and generalised strain measure. Magnesium material disk requires higher value of angular speed to yield at the inner surface as compared to the disk made of beryl material. With the effect of mechanical loading, angular speed also increases at the inner surface of the disk made of magnesium/beryl. Upon the introduction of mechanical loading, the rotating disk made of beryl material requires maximum radial stress at the inner surface as compared to disk made of magnesium material. The beryl material disk is more convenient than that of magnesium material.

INTRODUCTION

Rotating disks play a very important role in many applications in mechanical, aerospace industries, and chemical processing, such as compressors, flywheels, turbo generators, high speed gear engines, compressors, sink fits, steam turbines, pumps, and computer disks, etc. Materials have been widely used in engineering and human health applications. The solutions of disks can be found in a large number of textbooks, /1-6/. Gurushankar /7/ discussed stresses in a rotationally symmetric nonhomogeneous anisotropic annular disk with variable thickness and density under a thermal effect. Ghose /8/ investigated thermal effect on the transverse vibration of a spinning disk with variable thickness parameter. Guven /9/ analysed the stress distribution of hyperbolic disk with shaft by using plane stress.

Thakur et al. /10-38/ have investigated rotating disk with different parameters by using generalised strain measure. The objective of this research is to investigate transversely isotropic elastoplastic behaviour in a mechanically loaded rotating disk by using transition theory and generalised strain measure.

Ključne reči

- naponi
- disk
- berilijum
- magnezijum
- ugaona brzina

Izvod

U radu je istraženo transverszalno izotropno elastoplastično ponašanje mehanički opterećenog rotirajućeg diska primenom teorije prelaznih napona i generalisane mere deformacije. Disk od magnezijuma zahteva veće vrednosti ugaone brzine za pojavu tečenja na unutrašnjoj površini u poređenju sa diskom izrađenim od berila. Istovremenim uticajem mehaničkog opterećenja takođe dolazi i do povećanja ugaone brzine na unutrašnjoj površini diska izrađenog od magnezijuma/berila. Uvođenjem mehaničkog opterećenja, rotirajući disk od berila zahteva maksimalni radijalni napon na unutrašnjoj površini u poređenju sa diskom izrađenim od magnezijuma. Disk od berila je inženjerski pogodniji od diska izrađenog od magnezijuma.

MATERIALS

In the present study, we are using minerals, e.g., magnesium. Magnesium is transversely isotropic, shiny, silver, or gray coloured metal that is light in weight and strong. It has a hexagonal crystalline structure, capable of being shaped or bent. Beryl is a transversely isotropic material. It is a mineral composed of beryllium aluminium silicate with the chemical formula $\text{Be}_3\text{Al}_2\text{Si}_6\text{O}_{18}$. Well known varieties of beryl include emerald and aquamarine. Common beryl, mined as beryllium, is found in small deposits in many countries, but the main producers are Russia, Brazil, and the United States.

BASIC GOVERNING EQUATION

Let us consider a thin disk with a central bore of inner/outer radii as r_i and r_o and made of transversely isotropic material (i.e., beryl/magnesium), as shown in Fig. 1. The disk is rotating about its axis with angular velocity ω at the inner surface and its density is assumed to be constant.

The stress-strain relation of the elastic isotropic material is given by Thakur et al. /27/:

$$\tau_{rr} = \frac{1}{n} \left(\frac{c_{11}c_{33} - c_{13}^2}{c_{33}} \right) \left[2 - \eta^n \{1 + (1+T)^n\} \right] - 2 \frac{C_{66}}{n} [1 - \eta^n],$$

$$\tau_{\theta\theta} = \frac{1}{n} \left(\frac{c_{11}c_{33} - c_{13}^2}{c_{33}} \right) \left[2 - \eta^n \{1 + (1+T)^n\} \right] - 2 \frac{C_{66}}{n} [1 - \eta^n (1+T)^n],$$

$$\tau_{r\theta} = \tau_{\theta z} = \tau_{zr} = \tau_{zz} = 0. \quad (1)$$

The equation of equilibrium is given:

$$\frac{d}{dr} (r\tau_{rr}) - \tau_{\theta\theta} + \rho\omega^2 r^2 = 0 \quad (2)$$

Transition points: using Eq.(1) in Eq.(2), we get:

$$\eta^{n+1} (1+T)^{n-1} \frac{dT}{d\eta} = \frac{\rho\omega^2 r^2 c_{33}}{(c_{11}c_{33} - c_{13}^2)} + \eta^n \frac{2C_{66}c_{33}}{n(c_{11}c_{33} - c_{13}^2)} \times [1 + nT - (1+T)^n - T\{1 + (1+T)^n\}], \quad (3)$$

where: $r\eta' = \eta T$ (T is a function of η and η is the function of r); $T \rightarrow \pm\infty$ (elastic to plastic state), and $T \rightarrow -1$ (plastic to creep state), /10-38/.

ELASTOPLASTIC DEFORMATION

The circumferential stress is given by Thakur et al. /27/,

$$\tau_{\theta\theta} = k_1 r \frac{2c_{66}c_{33}}{c_{13}^2 - c_{11}c_{33}}. \quad (4)$$

Substituting Eq. (4) into Eq. (2), we get:

$$\tau_{rr} = \frac{k_2}{r} + k_1 \frac{r^{-2c_{66}c_{33}/(c_{13}^2 - c_{11}c_{33})}}{1 - \left(\frac{2c_{66}c_{33}}{c_{13}^2 - c_{11}c_{33}} \right)} - \frac{\rho\omega^2 r^2}{3}. \quad (5)$$

Substituting Eqs.(4)-(5) into the second Eq.(1), we get:

$$\eta = \sqrt{1 - \frac{2(c_{11}c_{33} - c_{13}^2 - 2c_{66}c_{33})}{E(c_{11}c_{33} - c_{13}^2)} \left[\frac{\rho\omega^2 r^2}{3} - \frac{k_2}{r} \right]}. \quad (6)$$

Substituting Eq.(6) into $u = r - r\eta$, /27/, we get:

$$u = r - r \sqrt{1 - \frac{2(c_{11}c_{33} - c_{13}^2 - 2c_{66}c_{33})}{E(c_{11}c_{33} - c_{13}^2)} \left[\frac{\rho\omega^2 r^2}{3} - \frac{k_2}{r} \right]}. \quad (7)$$

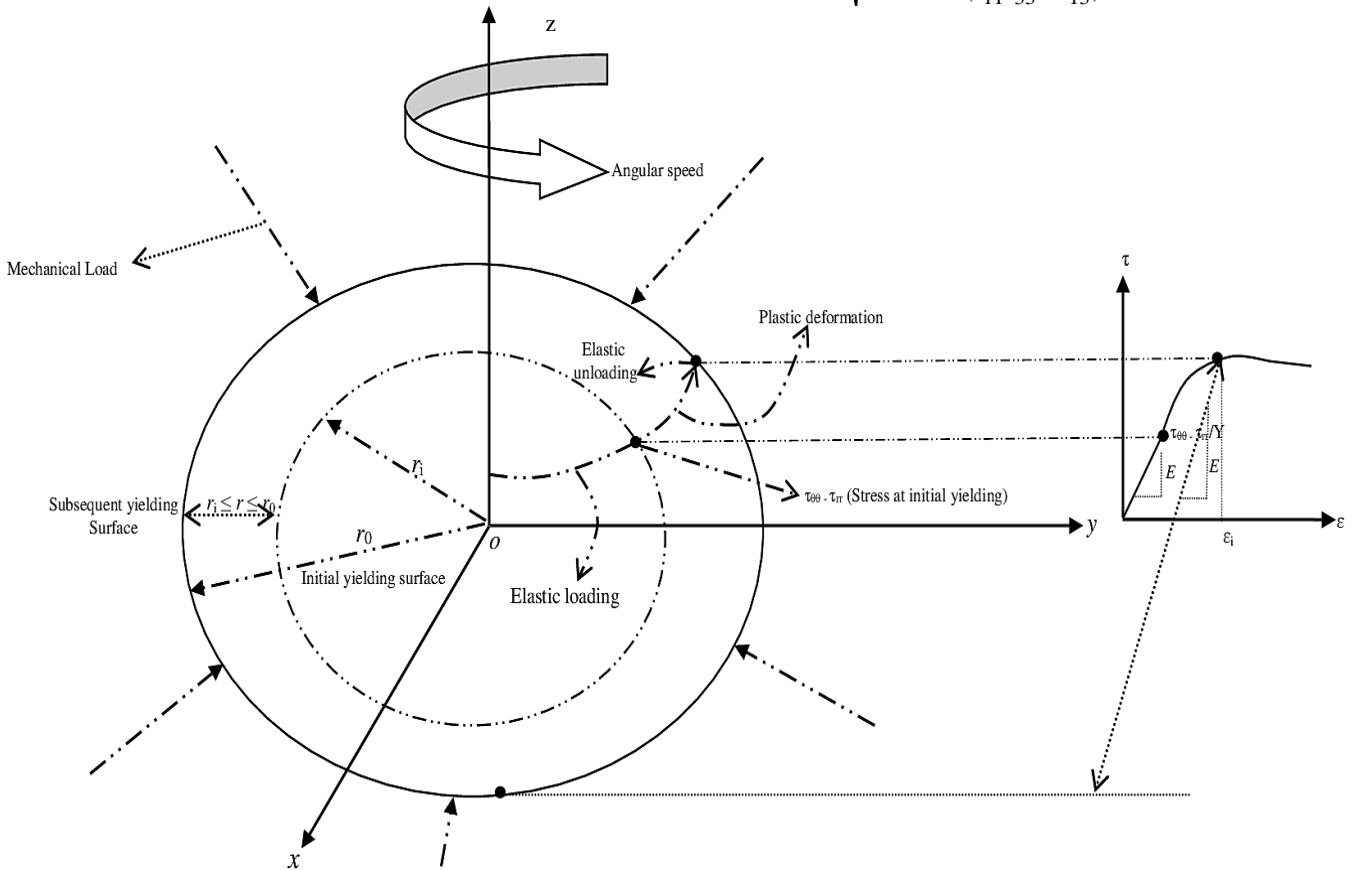


Figure 1. Geometry of disk.

where: $E = 2c_{66} \left(2 - \frac{2c_{66}c_{33}}{c_{13}^2 - c_{11}c_{33}} \right)$ is Young's modulus.

Using $\tau_{rr} = L_0$ at $r = r_0$, and $u = 0$ and $r = r_0$ in Eqs.(5) and (7) we get:

$$k_2 = \frac{\rho\omega^2 r_i^2}{3}, \text{ and}$$

$$k_1 = \frac{c_{11}c_{33} - c_{13}^2 - 2c_{66}c_{33}}{-\frac{2c_{66}c_{33}}{c_{13}^2 - c_{11}c_{33}}} \left[L_0 + \frac{\rho\omega^2}{3r_0} (r_0^3 - r_i^3) \right].$$

Substituting k_1 and k_2 in Eqs.(4), (5), and (7), we get

$$\tau_{\theta\theta} = \frac{c_{11}c_{33} - c_{13}^2 - 2c_{66}c_{33}}{c_{11}c_{33} - c_{13}^2} \left[L_0 + \frac{\rho\omega^2}{3r_0} (r_0^3 - r_i^3) \right] \left(\frac{r}{r_0} \right)^{\frac{2c_{66}c_{33}}{c_{13}^2 - c_{11}c_{33}}} \quad (8)$$

$$\tau_{rr} = \frac{\rho\omega^2}{3r} \left[(r_0^3 - r_i^3) \left(\frac{r}{r_0} \right)^{\frac{c_{11}c_{33} - c_{13}^2 - 2c_{66}c_{33}}{c_{11}c_{33} - c_{13}^2}} + r_i^3 - r^3 \right] + L_0 \left(\frac{r}{r_0} \right)^{-2c_{66}c_{33}/(c_{13}^2 - c_{11}c_{33})}, \quad (9)$$

and

$$u = r - r \sqrt{1 - \frac{2(c_{11}c_{33} - c_{13}^2 - 2c_{66}c_{33})\rho\omega^2(r^3 - r_i^3)}{3Er(c_{11}c_{33} - c_{13}^2)}}. \quad (10)$$

From Eqs.(8)-(9), we get:

$$\tau_{rr} - \tau_{\theta\theta} = \frac{\rho\omega^2}{3} \left[(1 - R_0^3)R \frac{c_{11}c_{33} - c_{13}^2 - 2c_{66}c_{33}}{c_{11}c_{33} - c_{13}^2} \frac{2c_{66}c_{33}}{c_{13}^2 - c_{11}c_{33}} + R_0^3 - R^3 \right] + L_0R \frac{2c_{66}c_{33}}{c_{13}^2 - c_{11}c_{33}}, \quad (11)$$

where: $R = r/r_0$ and $R_0 = r_i/r_0$.

Initial yielding surface: from Eq.(11) it is seen that $|\tau_{\theta\theta} - \tau_{rr}|$ is maximal at $R = R_0$, so yielding of the surface becomes:

$$|\tau_{\theta\theta} - \tau_{rr}|_{R=R_0} = \left| \frac{\rho\omega^2(1 - R_0^3)}{3} R \frac{c_{11}c_{33} - c_{13}^2 - 2c_{66}c_{33}}{c_{11}c_{33} - c_{13}^2} \frac{2c_{66}c_{33}}{c_{13}^2 - c_{11}c_{33}} + L_0R \frac{2c_{66}c_{33}}{c_{13}^2 - c_{11}c_{33}} \right| = Y, \text{ and angular speed for initial yielding surface are given:}$$

$$\Omega_i^2 = \left| \frac{3}{(1 - R_0^3)c_2R \frac{c_{11}c_{33} - c_{13}^2 - 2c_{66}c_{33}}{c_{11}c_{33} - c_{13}^2}} - \sigma_0 \frac{3}{(1 - R_0^3)R \frac{c_{11}c_{33} - c_{13}^2 - 2c_{66}c_{33}}{c_{11}c_{33} - c_{13}^2}} \right|, \quad (12)$$

where: $L_0/Y = \sigma_0$; and $\omega_i = (\Omega_i/r_0)\sqrt[4]{(Y/\rho)}$.

Subsequent yielding surface: from Eq.(11) $|\tau_{\theta\theta} - \tau_{rr}|$ is maximum at $R = 1$ and $\nu = 0.5$ for fully-plastic state, therefore yielding of the subsequent surface becomes:

$$|\tau_{\theta\theta} - \tau_{rr}|_{R=1} = \left| \frac{\rho\omega^2(1 - R_0^3)}{6} + \frac{\sigma_0}{2} \right| = Y; \text{ and angular speed for subsequent yielding surface becomes:}$$

$$\Omega_f^2 = \left| \frac{6}{(1 - R_0^3)} \left(1 - \frac{\sigma_0}{2} \right) \right|. \quad (13)$$

Stresses and displacement for initial yielding surface: from Eqs.(8)-(10), we get:

$$\sigma_\theta = \frac{c_{11}c_{33} - c_{13}^2 - 2c_{66}c_{33}}{c_{11}c_{33} - c_{13}^2} \left[\sigma_0 + \frac{\Omega_i^2}{3}(1 - R_0^3) \right] R \frac{2c_{66}c_{33}}{c_{13}^2 - c_{11}c_{33}}$$

$$\sigma_r = \frac{\Omega_i^2}{3R} \left[(1 - R_0^3)R \frac{c_{11}c_{33} - c_{13}^2 - 2c_{66}c_{33}}{c_{11}c_{33} - c_{13}^2} + R_0^3 - R^3 \right] + \sigma_0R \frac{2c_{66}c_{33}}{c_{13}^2 - c_{11}c_{33}}$$

$$\text{and } U = R - R \sqrt{1 - \frac{(c_{11}c_{33} - c_{13}^2 - 2c_{66}c_{33})H\Omega_i^2(R^3 - R_0^3)}{3R(c_{11}c_{33} - c_{13}^2)}}. \quad (14)$$

Stresses and displacement for subsequent yielding surface: by taking $\frac{2c_{66}c_{33}}{c_{13}^2 - c_{11}c_{33}} \rightarrow 0$ for fully-plastic state, Eqs.(8)-(10) are:

$$\sigma_\theta = \frac{1}{2\sqrt{R}} \left[\sigma_0 + \frac{\Omega_f^2}{3}(1 - R_0^3) \right],$$

$$\sigma_r = \frac{\Omega_f^2}{3R} \left[(1 - R_0^3)\sqrt{R} + R_0^3 - R^3 \right] + \frac{\sigma_0}{\sqrt{R}},$$

$$\text{and } U = R - R \sqrt{1 - \frac{H\Omega_f^2(R^3 - R_0^3)}{3R}}. \quad (15)$$

Validation of results: Eqs.(14)-(15) show similar results after neglecting thermal gradient, Thakur et al. /27/.

RESULTS AND DISCUSSION

To see the combined effect of stresses, mechanical load and angular speed in a disk made of transversely isotropic material, say magnesium (for $(2c_{66}c_{33})/(c_{13}^2 - c_{11}c_{33}) = 0.64$) and beryl ($(2c_{66}c_{33})/(c_{13}^2 - c_{11}c_{33}) = 0.69$) /27/, for the initial/subsequent yielding surface based on the following numerical values taken as: $r_i = 1$, $r_0 = 2$, and mechanical load $\sigma_0 = 0$ and 2, respectively.

Curves are drawn in Fig. 2 between angular speed Ω_i^2 versus radii ratio $R_0 = r_i/r_0$ for initial yielding surface. It is observed that magnesium material disk requires a higher value of angular speed to yield at the inner surface as compared to the disk made of beryl material. With the effect of mechanical loading, angular speed also increases at the inner surface of the disk made of magnesium/beryl.

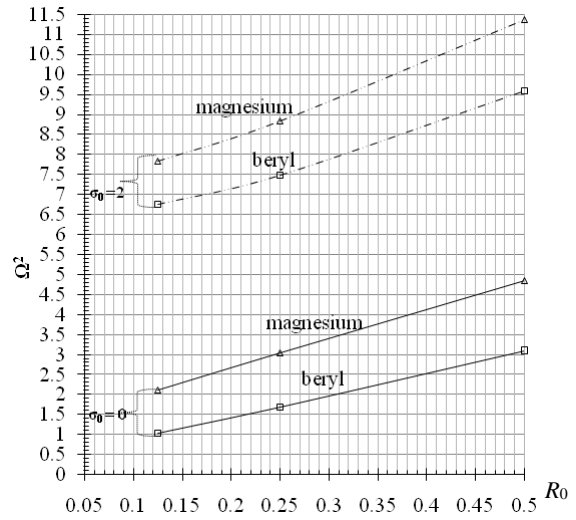
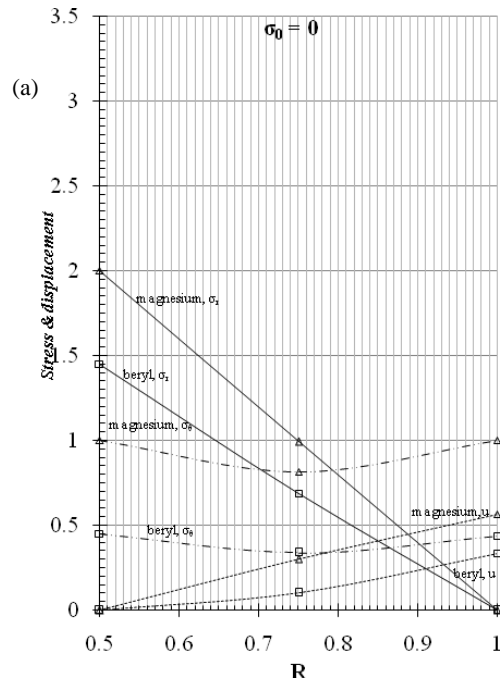


Figure 2. Graph between Ω_i^2 vs. R_0 .



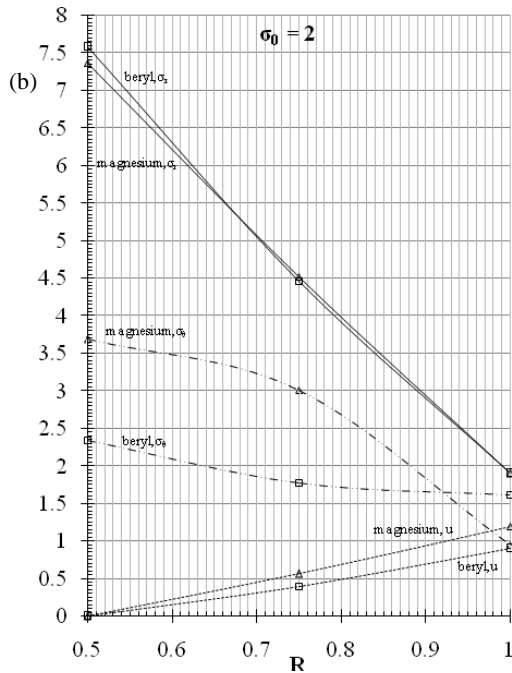


Figure 3. Stress distribution (a), and displacement (b), vs. radius.

In Fig. 3, curves are plotted between stress and displacement distribution versus radius ratio $R = r/r_0$. It has been seen that the rotating disk of magnesium material requires maximal value of radial stress at the inner surface in comparison to the disk of beryl material. By the introduction of mechanical loading, the rotating disk of beryl material requires maximal radial stress at the inner surface as compared to the disk of magnesium material at the internal surface, but at the intermediate surface, inverse results are obtained. Moreover, the rotating disk made of magnesium material is on the safer side of the design as compared to the disk made of beryl material, but reverse results are obtained by applying mechanical loading $\sigma_0 = 2$.

CONCLUSIONS

- The main findings can be concluded as follows.
- Magnesium material disk requires higher value of angular speed to yield at the inner surface as compared to the disk of beryl material. With the effect of mechanical loading, angular speed also increases at the inner surface of the disk made of magnesium/beryl.
- The rotating disk of magnesium material requires maximal value of radial stress at the inner surface compared to the disk of beryl material. The rotating disk of magnesium material requires higher value of radial stress at the internal surface in comparison to the disk of beryl material.
- By introducing mechanical loading, the rotating disk of beryl material requires maximum radial stress at the inner surface as compared to disk of magnesium material at the internal surface, but at the intermediate surface, inverse results are obtained. Moreover, the rotating disk of magnesium material is on the safer side of the design as compared to beryl material disk, but reverse results are obtained by apply the mechanical loading, $\sigma_0 = 2$.
- The disk of beryl material is more convenient than that of magnesium material.

REFERENCES

1. Timoshenko, S.P., Goodier, J.N., Theory of Elasticity, Third Ed., Mc Graw-Hill Book Co. New York, London, 1951.
2. Blazynski, T.Z., Applied Elasto-Plasticity of Solids, McMillan Press Ltd., London, 1983.
3. Johnson, W., Mellor, P.B., Plasticity for Mechanical Engineers, 1st Ed., D. Van-Nostrand Reinhold Inc., London, 1962.
4. Chakrabarty, J., Theory of Plasticity, McGraw-Hill, New York, 1987.
5. Sokolnikoff, I.S., Mathematical Theory of Elasticity, 2nd Ed., McGraw-Hill Inc., New York, 1953.
6. Heyman J., (1958), *Plastic design of rotating discs*, Proc. Inst. Mech. Eng. 172(1): 531-547. doi: 10.1243/PIME_PROC_1958_172_045
7. Gurushankar, G.V. (1975), *Thermal stresses in a rotating, non-homogeneous, anisotropic disk of varying thickness and density*, J Strain Anal. Eng. Des. 10(3): 137-142. doi: 10.1243/03093247V1031
8. Ghosh, N.C. (1975), *Thermal effect on the transverse vibration of spinning disk of variable thickness*, J Appl. Mech. 42(2): 358-362. doi: 10.1115/1.3423581
9. Güven, U. (1998), *Elastic-plastic stress distribution in a rotating hyperbolic disk with rigid inclusion*, Int. J Mech. Sci. 40(1): 97-109. doi: 10.1016/S0020-7403(97)00036-2
10. Gupta, S.K., Thakur, P. (2007), *Thermo elastic-plastic transition in a thin rotating disc with inclusion*, Therm. Sci. 11(1): 103-118. doi: 10.2298/TSCI0701103G
11. Thakur, P. (2010), *Elastic-plastic transition stresses in a thin rotating disc with rigid inclusion by infinitesimal deformation under steady-state temperature*, Therm. Sci. 14(1): 209-219. doi: 10.2298/TSCI1001209P
12. Thakur, P., Singh, S.B., Kaur, J. (2014), *Elastic-plastic stresses in a thin rotating disk with shaft having density variation parameter under steady-state temperature*, Kragujevac J Sci. 36: 5-17.
13. Thakur, P., Singh, S.B., Lozanović Šajic, J. (2015), *Thermo elastic-plastic deformation in a solid disk with heat generation subjected to pressure*, Struct. Integr. Life, 15(3): 135-142.
14. Kaur, J., Thakur, P., Singh, S.B. (2016), *Steady thermal stresses in a thin rotating disc of finitesimal deformation with mechanical load*, J Solid Mech. 8(1): 204-211.
15. Thakur, P., Kumar, S., Singh, J. (2017), *Creep stresses in a rotating disc having variable density and mechanical load under steady-state temperature*, Struct. Integr. Life, 17(2): 97-104.
16. Thakur, P., Gupta, N., Singh, S.B. (2017), *Creep strain rates analysis in cylinder under temperature gradient materials by using Seth's theory*, Eng. Comput. 34(3): 1020-1030. doi: 10.1108/EC-05-2016-0159
17. Thakur, P., Mahajan, P., Kumar, S. (2018), *Creep stresses and strain rates for a transversely isotropic disc having the variable thickness under internal pressure*, Struct. Integr. Life, 18 (1): 15-21.
18. Thakur, P., Sethi, M., Shahi, S., et al. (2018), *Modelling of creep behaviour of a rotating disc in the presence of load and variable thickness by using Seth transition theory*, Struct. Integr. Life, 18(2): 135-142.
19. Sethi, M., Thakur, P., Singh, H.P. (2019), *Characterization of material in a rotating disc subjected to thermal gradient by using Seth transition theory*, Struct. Integr. Life, 19(3): 151-156.
20. Thakur, P., Sethi, M. (2019), *Lebesgue measure in an elasto-plastic shell*, Struct. Integr. Life, 19(2): 115-120.
21. Sethi, M. Thakur P. (2020), *Elastoplastic deformation in an isotropic material disk with shaft subjected to load and variable density*, J Rubber Res. 23: 69-78. doi: 10.1007/s42464-020-00038-8

22. Thakur, P., Gupta N., Sethi, M., Gupta K. (2020), *Effect of density parameter in a disk made of orthotropic material and rubber*, J Rub. Res. 23(3): 193-201. doi: 10.1007/s42464-020-00049-5
23. Temesgen, A.G., Singh, S.B., Thakur, P. (2020), *Modelling of elastoplastic deformation of transversely isotropic rotating disc of variable density with shaft under a radial temperature gradient*, Struct. Integr. Life, 20(2): 113-121.
24. Thakur, P., Chand, S., Sukhvinder et al. (2020), *Density parameter in a transversely and isotropic disc material with rigid inclusion*, Struct. Integr. Life, 20(2): 159-164.
25. Thakur, P., Gupta, N., Gupta, K., Sethi, M. (2020), *Elastic-plastic transition in an orthotropic material disk*, Struct. Integr. and Life, 20(2): 169-172.
26. Thakur, P., Gupta N., Sethi, M., Gupta K. (2020), *Effect of density parameter in a disk made of orthotropic material and rubber*, J Rub. Res. 23(3): 193-201. doi: 10.1007/s42464-020-00049-5
27. Thakur, P., Kumar, N., Sethi, M. (2021), *Elastic-plastic stresses in a rotating disc of transversely isotropic material fitted with a shaft and subjected to thermal gradient*, Meccanica, 56: 1165-1175. doi: 10.1007/s11012-021-01318-2
28. Thakur, P., Sethi, M., Gupta, N., Gupta, K. (2021), *Thermal effects in rectangular plate made of rubber, copper and glass materials*, J Rubber Res. 24(1): 147-155. doi: 10.1007/s42464-020-00080-6
29. Temesgen, A.G., Singh, S.B., Thakur, P. (2021), *Elastoplastic analysis in functionally graded thick-walled rotating transversely isotropic cylinder under a radial temperature gradient and uniform pressure*, Math. Mech. Solids, 26(1): 5-17. doi: 10.1177/1081286520934041
30. Kumar, N., Thakur, P. (2021), *Thermal behaviour in a rotating disc made of transversely isotropic material with rigid shaft*, Struct. Integr. Life, 21(3): 217-223.
31. Thakur, P., Sethi, M., Kumar, N., et al. (2021), *Analytical solution of hyperbolic deformable disk having variable density*, Mech. Solids, 56(6): 1039-1046. doi: 10.3103/S0025654421060194
32. Thakur, P., Sethi, M., Gupta, K., Bhardwaj, R.K. (2021), *Thermal stress analysis in a hemispherical shell made of transversely isotropic materials under pressure and thermo-mechanical loads*, J Appl. Math. Mech. (ZAMM), 101(12). doi: 10.1002/zamm.202100208
33. Thakur, P., Sethi, M., Kumar, N., et al. (2021), *Thermal effects in a rotating disk made of rubber and magnesium materials and having variable density*, J Rubber Res. 24(3): 403-413. doi: 10.1007/s42464-021-00107-6
34. Thakur, P., Sethi, M., Kumar, N., et al. (2022), *Stress analysis in an isotropic hyperbolic rotating disk fitted with rigid shaft*, Z Angew. Math. Phys. 73(1), Art. ID 23. doi: 10.1007/s00033-021-01663-y
35. Thakur, P., Kumar, N., Gupta, K. (2022), *Thermal stress distribution in a hyperbolic disk made of rubber/brass material*, J Rub. Res. 25(1): 27-37. doi: 10.1007/s42464-022-00147-6
36. Gupta, K., Thakur, P., Bhardwaj, R.K. (2022), *Elasto-plastic stress analysis in a tube made of isotropic material and subjected to pressure and mechanical load*, Mech. Solids, 57(3): 617-628. doi: 10.3103/S002565442203013X
37. Chand S., Sood, S., Thakur, P., Gupta, K. (2023), *Elastoplastic stress deformation in an annular disk made of isotropic material and subjected to uniform pressure*, Struct. Integr. Life, 23(1): 61-64.
38. Singh, N., Kaur, J., Thakur, P., Murali, G. (2023), *Structural behaviour of annular isotropic disk made of steel/copper material with gradually varying thickness subjected to internal pressure*, Struct. Integr. Life, 23(3): 293-297.

© 2024 The Author. Structural Integrity and Life, Published by DIVK (The Society for Structural Integrity and Life 'Prof. Dr Stojan Sedmak') (<http://divk.inovacionicentar.rs/ivk/home.html>). This is an open access article distributed under the terms and conditions of the [Creative Commons Attribution-NonCommercial-NoDerivatives 4.0 International License](#)